New Heteromultifunctional Fluoroaromatic Bis(phosphinimine) Ligands and Their Complexes. Synthesis and Characterization of New Ligands (Including X-ray Structures of 4,6-$(CN)_2C_6F_2$-1-(N=P$(Ph)_2CH_2PPh_2$)-3-(N=PPh_3) and 4,6-$(CN)_2C_6F_2$-1,3-bis(N=P$(Ph)_2CH_2PPh_2$)) and Their Rhodium(I) Complexes, Including the Structure of the Novel Dimetallic Complex 4,6-$(CN)_2C_6F_2$-1,3-bis(N=P$(Ph)_2CH_2P(Ph)_2$Rh(CO)Cl)

Jin Li, Robert McDonald, and Ronald G. Cavell*

Department of Chemistry, University of Alberta, Edmonton, AB, Canada T6G 2G2

Received September 26, 1995[⊗]

Reaction of 1,3-dicyanotetrafluorobenzene with trimethylsilyl phosphinimines proceeds through stepwise substitution on the fluoroaromatic to yield mono- and ultimately disubstituted derivatives of the form 4,6-$(CN)_2C_6F_2$-1-A-3-B. Two molar equivalents of a bifunctional phosphinophosphoranimines, $Me_3SiNP(Ph)_2CH_2PPh_2$, result in a dual substitution giving **1** (A = B = (N=P$(Ph)_2CH_2PPh_2$)), whereas 1 equiv of the trimethylsilyl phosphinimine gives the monosubstituted derivative. Treatment of the monosubstituted derivative with a second 1 equiv of the same or a different phosphinimine gives doubly substituted derivatives which can have the same or different phosphorus substituents, e.g. **2**, A = (N=P$(Ph)_2CH_2P(Ph)_2$), B = (N=PPh_3), and **3**, A = (N=P$(Ph)_2CH_2PPh_2$), B = (N=PPh_2-Me). Compounds **1**, 4,6-$(CN)_2C_6F_2$-1,3-bis(N=P$(Ph)_2CH_2PPh_2$), and **2**, 4,6-$(CN)_2C_6F_2$-1-(N=P$(Ph)_2CH_2PPh_2$)-3-(N=PPh_3), have been structurally characterized. In **1**, the P(1)=N(1) bond length is 1.581(3) Å, the P(3)=N(2) bond length is 1.569(4) Å, the P(1)−N(1)−C(6) angle is 132.1(3)°, and the P(3)−N(2)−C(2) angle is 133.2(3)°. For **2**, the P(2)=N(1) bond length (in the Ph_3P=N unit) is 1.578(4) Å, the P(3)=N(2) bond length in the $Ph_2PCH_2Ph_2P$=N unit) is 1.585(4) Å, the P(2)−N(1)−C(2) angle is 134.7(4)°, and the P(3)−N(2)−C(6) angle is 129.9-(4)°. **2** reacted readily with $[Rh(CO)_2Cl]_2$ to form the mono metallic chelated Rh complex **4**, 4,6-$(CN)_2C_6F_2$-3-(N=PPh_3)-1-(N=P$(Ph)_2CH_2P(Ph)_2$Rh(CO)Cl). **1** reacts with both 1 equiv and 0.5 equiv of $[Rh(CO)_2Cl]_2$ to form respectively 4,6-$(CN)_2C_6F_2$-1,3-bis(N=P$(Ph)_2CH_2P(Ph)_2$Rh-(CO)Cl), **5**, and 4,6-$(CN)_2C_6F_2$-1,3-bis(N=P$(Ph)_2CH_2P(Ph)_2$)Rh(CO)Cl, **6**. The half-metalated complex **6** can be converted to **5** with a second aliquot of the Rh precursor, and the dimetalated complex **5** can be converted to the half-metalated complex **6** by reaction of **5** with more ligand. The bis(phosphine) chelate structure of **6**, the dimetalated complex, was deduced from the complex second-order ^{31}P NMR spectrum solved by simulation. The two P^{III} are *trans* coordinated to the Rh center, and the two N are not coordinated. There is no $P^{III}-P^{III}$ or $P^{V}-P^{V}$ coupling, but each P^{III} is coupled to two magnetically inequivalent P^{V}. Structural characterization of the dimetalated complex **5** shows a symmetrically substituted complex containing two Rh centers with a square planar geometry around each Rh(I) with the CO *cis* to the phosphine. Bond angles and lengths are typical for the Rh(I) square planar chelate complex structures. The P(1)−N(1) distance of 1.61(1) Å in the complex is normal for a coordinated iminophosphoranyl group. The directly bound Rh−P^{III} distance of 2.206-(4) Å also lies within the range found in many Rh(I) phosphine complexes of this type.

Introduction

We recently reported that silylated heterodifunctional phosphine-phosphinimines[1] (Scheme 1) could be easily converted to imino fluoroaromatic derivatives by a substitution on the imine center and that such species were effective ligands for binding both the early and the late transition metals.[2]

In the previous work, only monosubstituted derivatives were obtained[2] from both the 1,2- and 1,4-dicyanofluoroaromatics. Herein we report that, when R is the 1,3-dicyanofluoroaromatic, the reaction yields a series of disubstituted derivatives, two of which have

[⊗] Abstract published in *Advance ACS Abstracts,* December 15, 1995.
(1) Katti, K. V.; Cavell, R. G. *Inorg. Chem.* **1989**, *28*, 413.
(2) Katti, K. V.; Santarsiero, B. D.; Pinkerton, A. A.; Cavell, R. G. *Inorg. Chem.* **1993**, *32*, 5919.

Scheme 1

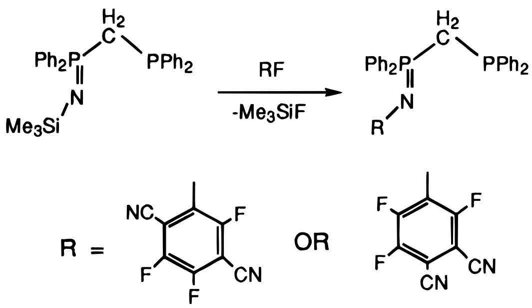

Scheme 2

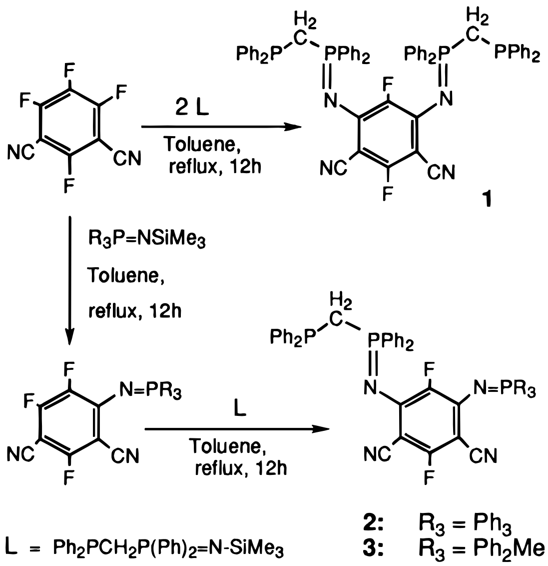

been structurally characterized. These multifunctional ligands also readily react with $[Rh(CO)_2Cl]_2$ to form mono- and dimetallic Rh(I) complexes, and one of the resultant complexes (the novel dimetallic derivative) has been structurally characterized.

Results and Discussion

Synthesis, Properties, and Structure. The reaction of 1,3-dicyanotetraflurobenzene with 2 equiv of trimethylsilyl phosphinimine in refluxing toluene gave the disubstituted fluoroaromatic derivatives **1**−**3** in good yield. In all cases fluorine atoms *para* to CN groups were replaced. Reactions proceeded smoothly with a 1:2 ratio of reagents to yield directly the equivalently disubstituted products or they could be carried out in a sequential stepwise fashion, that is, using initially 1 equiv of $R_3P{=}NSiMe_3$ to form the monosubstituted derivative and then using a second 1 equiv of either the same or a different silyl phosphinimine to form the disubstituted derivative. The silyl iminophosphorus reactant may be either a simple iminophosphorane, $R_3P{=}NSiMe_3$, or the more complex bifunctional iminophosphorano phosphines such as $Ph_2PCH_2PPh_2{=}N$-$SiMe_3$[1] (Scheme 2).

Two of these disubstituted ligands, **1** and **2**, have been structurally characterized. Both mono- and disubstituted fluoroaromatic compounds are crystalline, air-stable solids which are soluble in most common organic solvents. The disubstituted compounds are less soluble than the monosubstituted analogs. In the reactions shown in Scheme 2, the two fluorine atoms which are

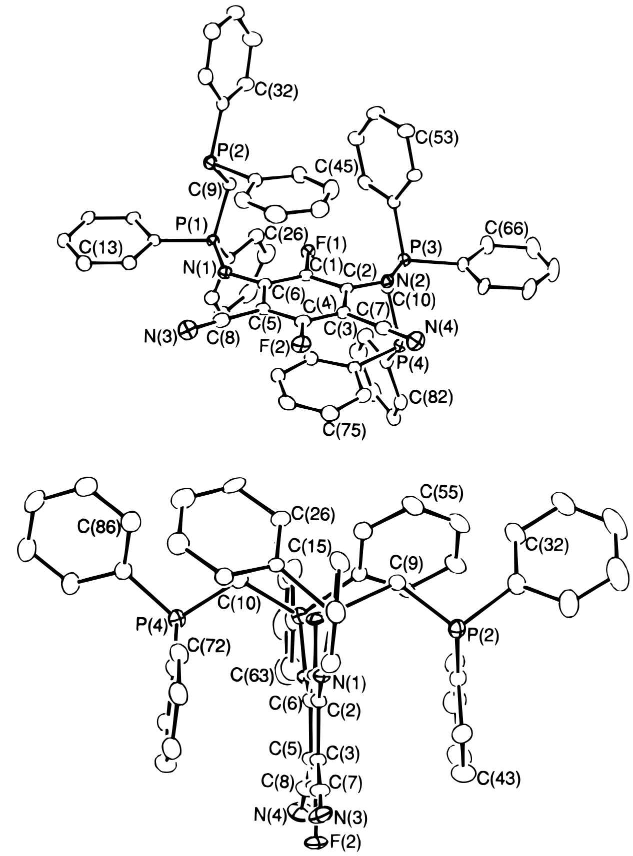

Figure 1. Top: Perspective views of **1** showing the atom-labeling scheme. Non-hydrogen atoms are represented by Gaussian ellipsoids at the 20% probability level. Hydrogen atoms are not shown. Bottom: Alternate view of the molecule with the C(1)−C(6) ring oriented almost edge-on.

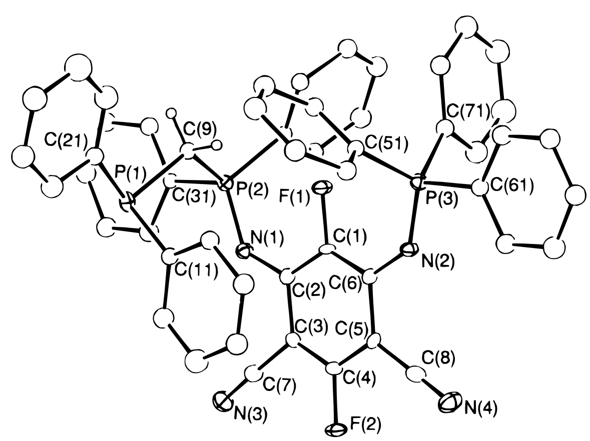

Figure 2. Perspective view of **2** showing the atom-labeling scheme. Non-hydrogen atoms are represented by Gaussian ellipsoids at the 20% probability level. The methylene hydrogens of the $N{=}PPh_2CH_2PPh_2$ group are shown artificially small, while those of the phosphine phenyl groups are not shown.

para to the electron-withdrawing activating groups, CN, in $1,3\text{-}(CN)_2C_6F_4$, are the most reactive and these fluorines are sequentially replaced. In contrast, only one of the fluorine atoms *para* to CN groups in $1,2\text{-}(CN)_2C_6F_4$ could be eliminated to form the imine and second substitution was not obtained,[2] because the first imine substitution electronically deactivates the *ortho* position.

Table 1. Phosphorus-31 NMR[a] Data for Compounds 1−6

compd[b]	no.	$\delta(P^{III})$ (ppm)	$\delta(P^{V})$ (ppm)	$^2J_{PP}$ (Hz)	$^1J_{PRh}$ (Hz)
4,6-$(CN)_2C_6F_2$-1,3-bis(N═$PPh_2CH_2PPh_2$)	**1**	−29.5	10.00	49.0	
4,6-$(CN)_2C_6F_2$-1-(N═$PPh_2CH_2PPh_2$)-3-(N═PPh_3)	**2**	−28.7	10.30 (PPh_2 unit), 8.40 (PPh_3 group)	47.8	
4,6-$(CN)_2C_6F_2$-1-(N═$PPh_2CH_2PPh_2$)-3-(N═PPh_2Me)	**3**	−29.2	10.30 (PPh_2 unit), 10.00 (PPh_2Me group)	48.4	
4,6-$(CN)_2C_6F_2$-3-(N═PPh_3)-1-(N═P(Ph)$_2$CH$_2$P(Ph)$_2$Rh(CO)Cl	**4**	39.2	44.00 (PPh_2 unit), 11.90 (PPh_3 group)	30.9	163.3
4,6-$(CN)_2C_6F_2$-1,3-bis(N═P(Ph)$_2$CH$_2$P(Ph)$_2$Rh(CO)Cl)	**5**	38.8	41.60	32.5	164.9
4,6-$(CN)_2C_6F_2$-1,3-bis(N═$PPh_2CH_2PPh_2$)Rh(CO)Cl	**6**	24.2	0.26	1.75,1.85	128.6

[a] Spectra obtained in $CDCl_3$ solution; ppm vs 85% H_3PO_4. Positive values indicate resonance to low field of standard. [b] The substituted aromatics are numbered starting from one at the imine attachment point. The numbers associated with the substituents may therefore be different from those used for the systematic name of the original fluroaromatic.

Table 2. Fluorine-19 NMR[a] Data and IR[b] Data for Compounds 1−6

compd	$\delta_{(F)}$[c] (ppm)	J_{FP} (Hz)	$^5J_{FF}$ (Hz)	ν_{CO} (cm^{-1})	ν_{CN} (cm^{-1})
1	F_2, −109.0 (dt); F_1, −140.7 (dt)	$^4J_{F1-P^V}$ = 14.0, $^5J_{F2-P^V}$ = 5.0	11.0		2205
2	F_2, −128.9 (a broad doublet); F_1, −138.9 (ddd)	$^4J_{F1-P1}$ = 14.3[d], $^4J_{F1-P2^V}$ = 13.8, $^5J_{F2-P1}$ = 5.0, $^5J_{F2-P2^V}$ = 4.7	11.3		2214
3	F_2, −108.9 (ddd); F_1, −141.5 (dddd)	$^4J_{F1-P1}$ = 14.6[d], $^4J_{F1-P2^V}$ = 13.9, $^5J_{F2-P1}$ = 5.0, $^5J_{F2-P2^V}$ = 4.4, $^4J_{F1-P^{III}}$ = 2.6	11.3		2214
4	F_2, −111.6 (dd); F_1, −141.5 (broad)	$^4J_{F1-P1}$ = 6.8[d], $^4J_{F1-P2^V}$ = 11.7, $^5J_{F2-P1}$ = 6.8, $^5J_{F2-P2^V}$ = 4.8	11.3	1970	2217
5	F_2, −106.4 (d); F_1, −119.2 (broad doublet)		11.3	1977	2227
6	F_2, −108.2 (dt); F_1, −136.4 (m)	$^6J_{F1-P^{III}}$ = 3.24, $^5J_{F1-P^V}$ = 8.92, $^5J_{F2-P^V}$ = 5.0	12.0	1972	2216

[a] Spectra obtained in $CDCl_3$ solution; ppm vs $CFCl_3$. Positive values indicate resonance to low field of standard. [b] All IR samples were run in CH_2Cl_2. [c] F_2 are adjacent to CN groups. [d] P_1 is in the unit of PPh_3 or PPh_2Me.

The identification and molecular constitution of all the compounds follows from the analytical data, mass spectra, and ^{1}H, ^{31}P, and ^{19}F NMR spectroscopy. Molecular ions for each of the compounds were observed in the mass spectra. Phosphorus-31 NMR data are given in Table 1, and the fluorine-19 NMR data are given in Table 2. The identity of chemical shifts for both P^{III} and both P^V atoms in compound **1** indicated that the two PCPN groups are related by symmetry. However when different phosphine imines are bound, the different environments are readily distinguished by their different chemical shifts. Compounds **1**−**3** also show characteristic $^2J_{PP}$ values which are about 5 Hz smaller than those obtained for analogous monosubstituted species.[2]

The crystal and molecular structures for **1** and **2** have been determined by X-ray diffraction as representative examples of these new ligands. The ORTEP[3] plots for **1** and **2** are shown in Figures 1 and 2, respectively.

The X-ray crystallographic data and the selected bonding parameters for these ligands are given in Tables 3−6 and in the Supporting Information. The structure of **1** shows considerable internal molecular regularity. The two remaining F atoms, the two CN groups, and the two imine N atoms are almost coplanar with the fluoroaromatic ring. One of the phenyl rings on each of the P^V centers is oriented approximately parallel to the fluoroaromatic ring (dihedral angles of 5.79 and 0.42°), and one of the phenyl rings on each of the P^{III} centers lies parallel to the fluoroaromatic ring and is arranged above and below the fluoroaromatic ring to form a sandwich of the fluoroaromatic ring with an eclipsed orientation (dihedral angles of 4.73 and 5.98°). In structure **2**, similar features are observed, and the dihedral angle is 3.7°. This eclipsed orientational structure is not uncommon in these molecular systems; similar relationships were previously observed in 4-(CN)-C_6F_4N═P(Ph)$_2$CH$_2$PPh$_2$ (where the dihedral angle is 19°) and 5-F-2,4-$(NO_2)_2C_6H_2$N═P(Ph)$_2$CH$_2$PPh$_2$ (where the dihedral angle is 8°).[2]

The X-ray crystallographic data for **1** and **2** further illuminate the nature of the P−N bond in the phosphoranimines, which is a polar, short bond of order greater than one.[4,5] Thus the P−N bond lengths in **1**, 1.569(4) and 1.581(3) Å, and in **2**, 1.585(4) Å (in the PCPN group) and 1.578(4) Å (in the Ph_3P═N group), are within the range of values for covalent radii (1.64 Å)[6] for a double bond and are comparable to those obtained for $[N(PPh_3)_2]^+$ (1.60 Å),[7] Ph_2FP═NMe (1.641 Å),[8] and Ph_3P═N-C_6H_4-*p*-Br (1.56 Å).[9] The P═N bond lengths observed in our compounds are however significantly longer than that in the prototypical precursor Me_3SiN═P-(Ph)$_2$CH$_2$PPh$_2$ (1.529(3) Å)[10] following the general trend of longer P═N bonds and narrower P−N−X angles for those iminophophoranes which carry organic substitutents (even those which are highly electron withdrawing) in contrast to those which have silyl substitutents.[11]

Complexation Reactions of 1 and 2 with [Rh(CO)$_2$Cl]$_2$. Compound **2** reacts with 0.5 equiv of $[Rh(CO)_2Cl]_2$ in CH_2Cl_2 at 25 °C to give complex **4** in high yield (Scheme 3).

The ^{31}P NMR chemical shifts of the P^{III} and P^V centers in complex **4** are very similar to those found earlier for

(3) Johnson, C. K. ORTEP, Report ORNL No. 5138, Oak Ridge National Laboratory, Oak Ridge, TN, 1976.

(4) Sudhakar, P. V.; Lammertsma, K. *J. Am. Chem. Soc.* **1991**, *113*, 1899.
(5) Johnson, A. W. *Ylides and Imides of Phosphorus*; Wiley: New York, 1993.
(6) Pauling, L. *The Nature of the Chemical Bond*, 3rd ed.; Cornell Univ Press: Ithaca, NY, 1960.
(7) Canziani, F.; Garlaschelli, L.; Malatesta, M. C.; Albinati, A. *J. Chem. Soc., Dalton Trans.* **1981**, 2395.
(8) Adamson, G. W.; Bart, J. C. J. *J. Chem. Soc. A* **1970**, 1452.
(9) Cameron, A. F.; Hair, N. S.; Norris, D. G. *Acta Crystallog., Sect. B* **1974**, *30*, 221.
(10) Schmidbaur, H.; Bowmaker, G. A.; Kumberger, O.; Müller, G.; Wolfsberger, W. *Z. Naturforsch. B* **1990**, *45b*, 476.
(11) Cavell, R. G.; Reed, R. W. Unpublished data.

Table 3. Summary of Crystallographic Data for Compounds 1, 2 and 5

compd	**1**	**2**	**5**
formula	$C_{62}H_{50}F_2N_6P_4$	$C_{53}H_{40}F_2N_5P_3$	$C_{62}H_{47}Cl_2F_2N_5O_2P_4Rh_2$
fw	1040.96	877.86	1332.71
cryst size (mm)	0.39 × 0.35 × 0.21	0.71 × 0.43 × 0.13	0.27 × 0.23 × 0.15
cryst system	triclinic	monoclinic	monoclinic
space group	$P\bar{1}$ (No. 2)	$P2_1/n^a$	$C2/c$ (No. 15)
unit cell params			
a (Å)	10.6203(6)	14.101(2)	25.158(9)
b (Å)	14.2626(6)	10.209(1)	16.379(2)
c (Å)	20.0527(8)	31.845(3)	18.723(6)
α (deg)	79.577(4)		
β (deg)	77.371(4)	99.38(1)	125.63(2)
γ (deg)	68.886(4)		
V (Å^3)	2747.5 (2)	4523 (1)	6271 (7)
Z	2	4	4
ρ_{calcd} (g cm^{-3})	1.258	1.289	1.412
μ (mm^{-1})	1.686	0.177	0.753
diffractometer	Siemens P4/RA	Enraf-Nonius CAD4	Enraf-Nonius CAD4
radiation (λ (Å))	Cu Kα (1.541 78)	Mo Kα (0.710 73)	Mo Kα (0.710 73)
temp (°C)	−60	−50	−50
scan type	$\theta-2\theta$	ω	$\theta-2\theta$
max 2θ (deg)	100.0	50.0	50.0
tot. data collcd	6823	8563	5852
indpdt reflcns (NR)	5635	8346	5710
observns (NO)	4473b	3097[c]	1950[c]
structure solution method	direct methods[d]	direct methods[d]	direct methods[d]
refinement method	full-matrix on F^2 [e]	full-matrix on F[f]	full-matrix on F[f]
abs corr method	DIFABS[g]	DIFABS[g]	DIFABS[g]
range of abs corr factors	1.348−0.805	1.084−0.731	1.251−0.764
params (NV)	667	343	234
goodness-of-fit (S)	1.053[h]	1.753[i]	1.549[i]
final R indices[j]			
R_1	0.0526[b]	0.064[c]	0.064[c]
R_2		0.071[c]	0.067[c]
wR_2	0.1426[k]		

[a] A nonstandard setting of $P2_1/c$ (No. 14). [b] $I \geq 2\sigma(I)$. [c] $I \geq 3\sigma(I)$. [d] Sheldrick, G. M. *Acta Crystallogr.* **1990**, *A46*, 467. [e] Sheldrick, G. M. *J. Appl. Crystallogr.* Manuscript in preparation. Refinement on F_o^2 for *all* reflections (all of these having $F_o^2 < -3\sigma(F_o^2)$). *R*-factors based on F_o^2 are statistically about twice as large as those based on F_o, and *R*-factors based on *all* data will be even larger. [f] *Structure Determination Package*, version 3; Enraf-Nonius: Delft, The Netherlands, 1985. [g] Walker, N.; Stuart, D. *Acta Crystallogr.* **1983**, *A39*, 158. [h] $S = [\Sigma w_2(F_o^2 - F_c^2)^2/(NR - NV)]^{1/2}$ ($w_2 = [\sigma^2(F_o^2) + (0.0677P)^2 + 2.8559P]^{-1}$, where $P = [\max(F_o^2,0) + 2F_c^2]/3$). [i] $S = [\Sigma w_1(|F_o| - |F_c|)^2/(NO - NV)]^{1/2}$ ($w_1 = 4F_o^2/\sigma^2(F_o^2)$). [j] $R_1 = \Sigma||F_o| - |F_c||/\Sigma|F_o|$; $R_2 = [\Sigma w_1(|F_o| - |F_c|)^2/\Sigma w_1 F_o^2]^{1/2}$; $wR_2 = [\Sigma w_2(F_o^2 - F_c^2)^2/\Sigma w_2(F_o^4)]^{1/2}$. [k] On all data.

Table 4. Selected Bond Distances (Å) in Compounds 1, 2 and 5

1		**2**		**5**	
P(1)−N(1)	1.581(3)	P(1)−C(9)	1.860(5)	Rh−Cl	2.361(4)
P(1)−C(9)	1.805(4)	P(1)−C(11)	1.826(5)	Rh−P(2)	2.206(4)
P(1)−C(11)	1.802(4)	P(1)−C(21)	1.831(6)	Rh−N(1)	2.153(8)
P(1)−C(21)	1.797(4)	P(2)−N(1)	1.585(4)	Rh−C(6)	1.426(3)
P(2)−C(9)	1.853(4)	P(2)−C(9)	1.807(5)	P(1)−N(1)	1.61(1)
P(2)−C(31)	1.833(5)	P(2)−C(31)	1.787(5)	P(1)−C(7)	1.78(1)
P(2)−C(41)	1.839(5)	P(2)−C(41)	1.802(5)	P(1)−C(11)	1.77(1)
P(3)−N(2)	1.569(4)	P(3)−N(2)	1.578(4)	P(1)−C(21)	1.81(1)
P(3)−C(10)	1.801(4)	P(3)−C(51)	1.803(5)	P(2)−C(7)	1.78(1)
P(3)−C(51)	1.806(4)	P(3)−C(61)	1.797(5)	P(2)−C(31)	1.79(1)
P(3)−C(61)	1.805(4)	P(3)−C(71)	1.798(6)	P(2)−C(41)	1.81(1)
P(4)−C(10)	1.858(4)	F(1)−C(1)	1.377(5)	F(1)−C(1)	1.36(2)
P(4)−C(71)	1.828(5)	F(2)−C(4)	1.373(6)	F(2)−C(4)	1.35(2)
P(4)−C(81)	1.827(5)	N(1)−C(2)	1.351(6)	O−C(6)	1.12(1)
F(1)−C(1)	1.366(4)	N(2)−C(6)	1.364(6)	N(1)−C(2)	1.40(1)
F(2)−C(4)	1.354(5)	N(3)−C(7)	1.143(6)	N(2)−C(5)	1.12(1)
N(1)−C(6)	1.358(5)	N(4)−C(8)	1.149(7)	C(3)−C(5)	1.46(2)
N(2)−C(2)	1.356(5)	C(3)−C(7)	1.448(7)		
N(3)−C(8)	1.140(6)	C(5)−C(8)	1.414(8)		
N(4)−C(7)	1.140(6)				
C(3)−C(7)	1.429(7)				
C(5)−C(8)	1.435(7)				

[a] Numbers in parentheses are estimated standard deviations in the least significant digits.

Table 5. Selected Bond Angles (deg) in Compound 1[a]

N(1)−P(1)−C(11)	105.4(2)	N(3)−C(7)−C(3)	179.2(5)
N(1)−P(1)−C(21)	115.8(2)	N(4)−C(8)−C(5)	178.8(5)
C(9)−P(1)−C(11)	106.4(2)	P(1)−C(9)−P(2)	110.2(2)
C(9)−P(1)−C(21)	108.7(2)	P(3)−C(10)−P(4)	110.7(2)
C(11)−P(1)−C(21)	103.5(2)	P(1)−C(11)−C(12)	121.0(3)
C(9)−P(2)−C(31)	101.3(2)	P(1)−C(11)−C(16)	119.6(3)
C(9)−P(2)−C(41)	102.1(2)	P(1)−C(21)−C(22)	116.4(3)
C(31)−P(2)−C(41)	100.9(2)	P(1)−C(21)−C(26)	125.4(3)
N(2)−P(3)−C(10)	116.4(2)	P(2)−C(31)−C(32)	127.0(4)
N(2)−P(3)−C(51)	114.3(2)	P(2)−C(31)−C(36)	115.3(4)
N(2)−P(3)−C(61)	105.0(2)	P(2)−C(41)−C(42)	117.2(4)
C(10)−P(3)−C(51)	109.2(2)	P(2)−C(41)−C(46)	124.4(4)
C(10)−P(3)−C(61)	106.3(2)	P(3)−C(51)−C(56)	125.4(3)
C(51)−P(3)−C(61)	104.5(2)	P(3)−C(51)−C(52)	116.1(3)
C(10)−P(4)−C(71)	102.0(2)	P(3)−C(61)−C(62)	121.1(4)
C(10)−P(4)−C(81)	101.6(2)	P(3)−C(61)−C(66)	118.4(4)
C(71)−P(4)−C(81)	101.7(2)	P(4)−C(71)−C(76)	118.3(4)
P(1)−N(1)−C(6)	132.1(3)	P(4)−C(71)−C(72)	123.8(4)
P(3)−N(2)−C(2)	133.2(3)	P(4)−C(81)−C(86)	125.8(4)
F(1)−C(1)−C(2)	116.8(3)	P(4)−C(81)−C(82)	115.8(4)
N(1)−C(2)−C(1)	127.5(4)	C(2)−C(3)−C(7)	119.3(4)
N(1)−C(2)−C(3)	116.8(4)	C(4)−C(3)−C(7)	121.8(4)
F(2)−C(4)−C(5)	118.6(4)	C(4)−C(5)−C(8)	121.0(4)
N(2)−C(6)−C(1)	127.5(4)	C(6)−C(5)−C(8)	118.6(4)
N(2)−C(6)−C(5)	118.0(4)		

[a] Numbers in parentheses are estimated standard deviations in the least significant digits.

the complexes $RN{=}P(Ph)_2CH_2P(Ph)_2Rh(CO)Cl$,[2,12] in which the imine nitrogen carries fluoroaromatic or dinitro substituents (R); however, in **4**, the signal arising from the uncomplexed $Ph_3P{=}N$ unit is shifted to low field by about 3.5 ppm suggesting some additional

(12) Cavell, R. G.; Katti, K. V. Unpublished data.

Table 6. Selected Bond Angles (deg) in Compound 2[a]

C(9)−P(1)−C(11)	101.3(2)	N(2)−C(6)−C(1)	127.4(5)
C(9)−P(1)−C(21)	100.6(2)	N(2)−C(6)−C(5)	116.3(5)
C(11)−P(1)−C(21)	99.2(2)	N(3)−C(7)−C(3)	177.6(7)
N(1)−P(2)−C(9)	115.5(3)	N(4)−C(8)−C(5)	178.9(7)
N(1)−P(2)−C(31)	106.1(3)	P(1)−C(9)−P(2)	110.5(3)
N(1)−P(2)−C(41)	114.7(3)	P(1)−C(11)−C(12)	123.4(4)
C(9)−P(2)−C(31)	104.5(2)	P(1)−C(11)−C(16)	119.5(4)
C(9)−P(2)−C(41)	109.3(2)	P(1)−C(21)−C(22)	114.6(5)
C(31)−P(2)−C(41)	105.7(2)	P(1)−C(21)−C(26)	126.9(5)
N(2)−P(3)−C(51)	116.0(2)	P(2)−C(31)−C(32)	122.0(4)
N(2)−P(3)−C(61)	104.5(3)	P(2)−C(31)−C(36)	118.9(4)
N(2)−P(3)−C(71)	116.8(3)	P(2)−C(41)−C(42)	114.9(4)
C(51)−P(3)−C(61)	104.7(2)	P(2)−C(41)−C(46)	124.2(4)
C(51)−P(3)−C(71)	108.5(3)	P(3)−C(51)−C(52)	125.4(4)
C(61)−P(3)−C(71)	105.0(3)	P(3)−C(51)−C(56)	115.5(4)
P(2)−N(1)−C(2)	129.9(4)	P(3)−C(61)−C(62)	120.4(4)
P(3)−N(2)−C(6)	134.7(4)	P(3)−C(61)−C(66)	120.3(4)
F(1)−C(1)−C(2)	116.2(5)	P(3)−C(71)−C(72)	115.9(5)
F(1)−C(1)−C(6)	116.1(4)	P(3)−C(71)−C(76)	124.4(5)
N(1)−C(2)−C(1)	128.8(5)	C(2)−C(3)−C(7)	119.5(5)
N(1)−C(2)−C(3)	117.4(5)	C(4)−C(3)−C(7)	120.6(5)
F(2)−C(4)−C(3)	117.8(5)	C(4)−C(5)−C(8)	121.9(5)
F(2)−C(4)−C(5)	116.9(5)	C(6)−C(5)−C(8)	121.1(5)

[a] Numbers in parentheses are estimated standard deviations in the least significant digits.

Scheme 3

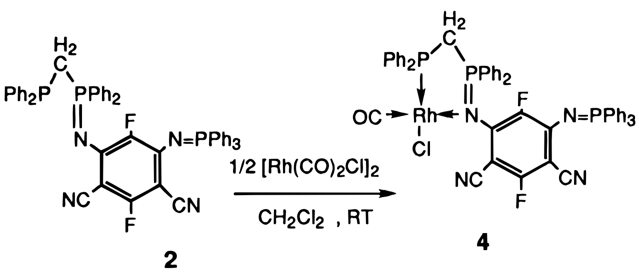

electron delocalization from the fluoroaromatic ring in this complex. Direct P^{III}−Rh bonding is clearly indicated by the large characteristic $^1J_{PRh}$ value. The ν_{CO} value of 1970 cm^{-1} (Table 2) indicates that the CO group coordinated to Rh is located *cis* to the P^{III} center.

Compound **1** reacts with 1 molar equiv of $[Rh(CO)_2Cl]_2$ to give the dimetallic complex **5** (Scheme 4) in which both coordination sites are occupied.

Reacting **1** with 0.5 equiv of $[Rh(CO)_2Cl]_2$ gives complex **6** in which only one Rh atom is complexed by the ligand (Scheme 4), and in turn, another 1 equiv of Rh precursor at room temperature in CH_2Cl_2 gives the fully metalated product **5.** The process can be reversed in that treating **5** with more ligand **1**, again at room temperature in CH_2Cl_2, produces the half-metalated product **6**.

The NMR data of **5** showed that the two Rh centers are equivalent with ^{31}P chemical shifts of the P^V and P^{III} centers being similar to those of the monosubstituted analogs. The P^{III} signal is strongly shifted (by 68 ppm) to low field upon coordination, and the P^V signal, a broad poorly resolved doublet, is similarly shifted (by 32 ppm) relative to the free ligand. The fluorine located between the two CN groups in **5** shows no substantial change in the NMR chemical shift upon complexation of the ligand to the metal, but the fluorine located between the imine nitrogens is shifted by 22 ppm to low field upon complex formation. The crystal structure (*vide infra*) shows that this fluorine is located very close to two of the phenyl groups, one from each of the two

Scheme 4

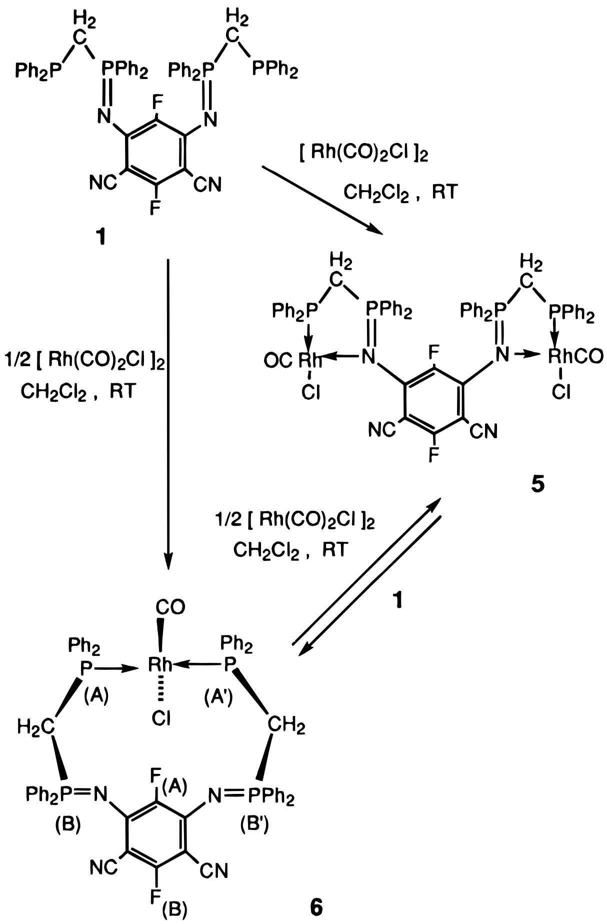

P^V centers, and the observed low-field shift probably reflects the deshielding by this phenyl group environment. Similar behavior was also observed in complex **4**. In that case, the ^{19}F chemical shifts of the fluorine atom which is located ortho to the P^V were shifted by 16 ppm to low field suggesting that one of the phenyl substituents on P^V lies physically close to this fluorine. The CO stretching frequency of **5** is 1979 cm^{-1}, consistent with a *cis* phosphine−carbonyl structure. The ^1H NMR spectrum in the CH_2 region showed two signals implying two inequivalent environments for the hydrogens of each methylene group.

The molecular structure of **5** was obtained by X-ray diffraction, and the ORTEP[3] plot is shown in Figure 3. The structural parameters for **5** and the bonding parameters are given in Tables 3, 4, and 7 and in Supporting Information. The structure comprises the neutral dimeric complex $4,6\text{-}(CN)_2C_6F_2\text{-}1,3\text{-bis}(N{=}P(Ph)_2\text{-}CH_2P(Ph)_2Rh(CO)Cl)$, **5**, with a cocrystallized molecule of CH_3CN. The complex shows a square planar geometry around each Rh(I) with the CO *cis* to the phosphine as indicated by the IR spectrum. Bond angles and lengths are typical for a square planar chelate of Rh(I). The P(1)−N(1) distance of 1.61(1) Å in the complex is within the range found for a coordinated iminophosphoranyl group.[2] The directly bound Rh−P^{III} distance of 2.206(4) Å also lies within the range found in many Rh(I) phosphine complexes of the type $P_2Rh(CO)Cl$.[13−19]

(13) Bennett, M. J.; Donaldson, P. B. *J. Am. Chem. Soc.* **1971**, *93*, 3307.

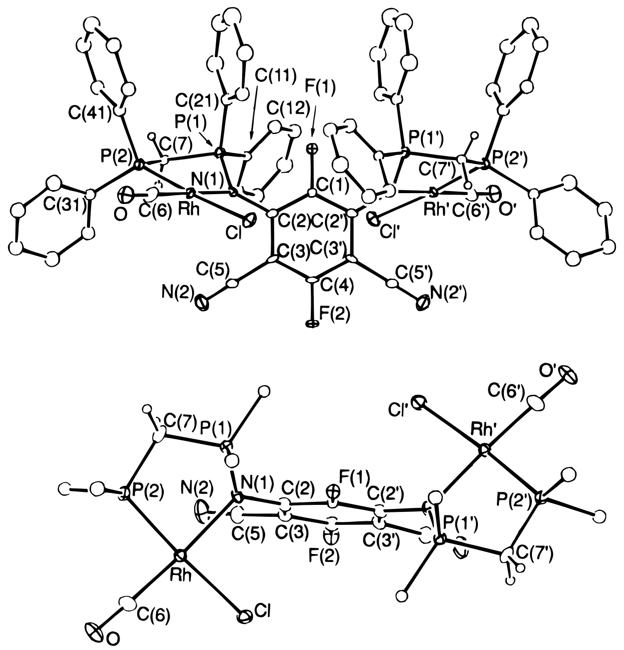

Figure 3. Top: Perspective views of **5** showing the atom-labeling scheme. Non-hydrogen atoms are represented by Gaussian ellipsoids at the 20% probability level. The dppm methylene hydrogens are shown artificially small, while those of the phosphine phenyl groups are not shown. Bottom: Top view of the molecule.

Table 7. Selected Bond Angles (deg) in Compound 5[a]

Cl−Rh−P(2)	174.7(1)	Rh−N(1)−C(2)	123.4(8)
Cl−Rh−N(1)	87.8(3)	P(1)−N(1)−C(2)	123.0(8)
Cl−Rh−C(6)	95.2(4)	F(1)−C(1)−C(2)	117.6(9)
P(2)−Rh−N(1)	87.7(3)	N(1)−C(2)−C(1)	124(1)
P(2)−Rh−C(6)	89.4(4)	N(1)−C(2)−C(3)	119(1)
N(1)−Rh−C(6)	176.4(5)	C(2)−C(3)−C(5)	121(1)
N(1)−P(1)−C(7)	101.8(5)	C(4)−C(3)−C(5)	121(1)
N(1)−P(1)−C(11)	113.2(5)	F(2)−C(4)−C(3)	117.9(8)
N(1)−P(1)−C(21)	114.6(6)	N(2)−C(5)−C(3)	176(2)
C(7)−P(1)−C(11)	110.7(6)	Rh−C(6)−O	178(1)
C(7)−P(1)−C(21)	106.2(5)	P(1)−C(7)−P(2)	108.5(6)
C(11)−P(1)−C(21)	109.9(5)	P(1)−C(11)−C(12)	118.9(9)
Rh−P(2)−C(7)	105.4(4)	P(1)−C(11)−C(16)	124(1)
Rh−P(2)−C(31)	116.4(4)	P(1)−C(21)−C(22)	119(1)
Rh−P(2)−C(41)	120.3(4)	P(1)−C(21)−C(26)	121(1)
C(7)−P(2)−C(31)	108.3(5)	P(2)−C(31)−C(32)	121(1)
C(7)−P(2)−C(41)	102.6(6)	P(2)−C(31)−C(36)	122.3(9)
C(31)−P(2)−C(41)	102.6(6)	P(2)−C(41)−C(42)	123(1)
Rh−N(1)−P(1)	111.2(5)	P(2)−C(41)−C(46)	120(1)

[a] Numbers in parentheses are estimated standard deviations in the least significant digits.

The molecule has C_2 symmetry with the two fluorine atoms and the carbons to which they are attached being located on a crystallographic 2-fold axis. These two F atoms, the two CN groups, and two imine N atoms are coplanar with the fluoroaromatic ring. The Cl, Rh, C(6), O, N(1), P(2) and C(7) atoms are almost coplanar, while P(1) lies significantly above the plane, by 0.722 Å. The dihedral angle between the Rh−P(2)−C(7)−N(1) and C(7)−P(1)−N(1) planes is 133.3°. The view shown in the lower structure of Figure 3 clearly shows that one Rh lies below and the other lies above the fluoroaromatic ring. The dihedral angle between the Rh−P(2)−C(7)−N(1) plane and the fluoroaromatic ring is 76.0°.

Compared with our previously described Rh complexes,[2,20,21] and the above described disubstituted complex, this Rh complex was unusual. First, ^{31}P NMR data indicate that the two PCPN groups are symmetrically coordinated to Rh; therefore, we surmise that the two P^{III} units must be coordinated to the Rh metal center and that they must be in a mutual *trans* relationship. The presence of a large coupling in the P^{III} unit due to $^{1}J_{PRh}$ readily identifies the ^{31}P chemical shift of P^{III} showing that this signal lies to lower field than that of P^{V}. Thus the P^{III} has shifted by about 54 ppm to low field upon coordination (as in **5** and **4**) whereas the P^{V} signal shifts instead to high field by about 10 ppm. The $^{1}J_{PRh}$ value of 128.6 Hz (obtained by analysis of the second-order spectrum) is also smaller than usual. For the ^{19}F NMR spectrum, the fluorine which lies between the two P^{V} imines is not as greatly affected as was the case in **5** and has only been shifted by 4 ppm to low field upon complexation. This suggests that in this case the phenyl rings subtended on P^{V} are not proximate to this fluorine as was the case with **4**. The spectral pattern is a doublet of triplets of triplets, which indicates coupling to the other fluorine, two P^{V} and two P^{III}, respectively. The other fluorine is a doublet of triplets, clearly arising from the coupling to one other fluorine and to two P^{V} but not to the remote P^{III}. The ^{31}P NMR spectrum was clearly second order and showed complex multiplets for both P^{III} and P^{V} signals. The spectral pattern for **6** is illustrated in Figure 4 (top). A large coupling between Rh and P^{III} is readily observed which clearly identifies this low-field signal as that arising from the P^{III} center. The P^{V} signal is therefore the higher field signal which contrasts to related compounds in the system but which is consistent with the proposed formulation. In this case the imine N of the PCPN unit is not coordinated to the Rh center and so the P^{V} signal is not substantially shifted by coordination. The coupling patterns cannot be clearly extracted even in spite of substantial but obscure P^{III}−P^{V} coupling which is usually a clearly defined feature in spectra of compounds of this type. Homonuclear ^{31}P-{^{31}P} NMR decoupling measurements (Figure 4, bottom) applied to P^{V} reduced the P^{III} pattern to a doublet of doublets, the smaller doublet probably arising from the coupling of F1 with P^{III}. Applied to P^{III}, homonuclear decoupling reduces the P^{V} pattern to a doublet of doublets which indicates that P^{V} couples to two different fluorines (Figure 4, bottom). These experiments in themselves did not provide sufficient information to fully determine the coupling interactions between P^{III} and P^{V}. The pattern of the spectrum was however successfully simulated (Figure 4, middle)[22] with the fit shown. The successful spectral simulation suggests that the two P^{III} centers and likewise the two P^{V} centers are each

(14) Bennett, M. J.; Donaldson, P. B. *Inorg. Chem.* **1977**, *16*, 1581.
(15) Bennett, M. J.; Donaldson, P. B. *Inorg. Chem.* **1977**, *16*, 1585.
(16) Bennett, M. J.; Donaldson, P. B. *Inorg. Chem.* **1977**, *16*, 655.
(17) Bonnet, J. J.; Kalck, P.; Poilblanc, R. *Inorg. Chem.* **1977**, *16*, 1514.
(18) Kessler, J. M.; Nelson, J. H.; Frye, J. S.; DeCian, A.; Fischer, J. *Inorg. Chem.* **1993**, *32*, 1048.
(19) Osakada, K.; Hataya, K.; Yamamoto, T. *Inorg. Chem.* **1993**, *32*, 2360.
(20) Katti, K. V.; Cavell, R. G. *Organometallics* **1988**, *7*, 2236.
(21) Katti, K. V.; Cavell, R. G. *Organometallics* **1989**, *8*, 2147.
(22) NMR spectral simulations were carried out with the Bruker Instrument Co. spectral analysis program, PANIC (parameter adjustment in NMR by iteration calculation). The simulated ^{31}P NMR spectrum parameters for compound **6** are as follows: $^{1}J_{P(A)-Rh}$ = $^{1}J_{P(A')-Rh}$ = 128.5 Hz, $^{2}J_{P(A)-P(B)}$ = $^{2}J_{P(A')-P(B')}$ = 1.85 Hz, $^{4}J_{P(A)-P(B')}$ = $^{4}J_{P(A')-P(B)}$ = 1.75 Hz, $^{6}J_{P(A)-F(A)}$ = $^{6}J_{P(A')-F(A)}$ = 3.24 Hz, $^{4}J_{P(B)-F(A)}$ = $^{4}J_{P(B')-F(A)}$ = 8.92 Hz, $^{5}J_{P(B)-F(B)}$ = $^{5}J_{P(B')-F(B)}$ = 5.00 Hz, $^{5}J_{F(A)-F(B)}$ = 12.00Hz.

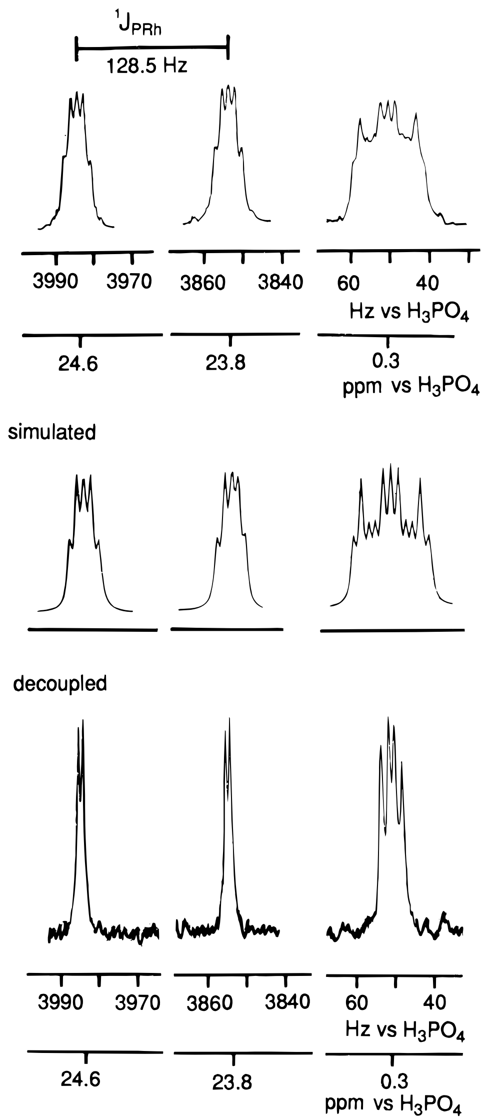

Figure 4. ^{31}P NMR spectra of **6**: (top) experimental spectrum; (center) simulated spectrum; Bottom: spectrum with homonuclear $^{31}P\{^{31}P\}$ decoupling applied to P^V and P^{III}, respectively.

chemically equivalent but the magnetical inequivalence leads to second order behavior. The coupling constants extracted from the simulation, $^2J_{P(A)-P(B)} = {}^2J_{P(A')-P(B')} = 1.85$ Hz and $^4J_{P(A)-P(B')} = {}^4J_{P(A')-P(B)} = 1.75$ Hz show only a very small difference (0.10 Hz) between each other, but we feel that the values are reliable because small changes in these coupling constant values make a big difference in the calculated spectral pattern and destroy the match with the experimental spectrum.

The ^{1}H NMR spectrum of the CH_2 region of **6**, similar to that for **5**, showed two different signals, each one showing a doublet of doublet of doublets pattern. The two hydrogens on each methylene carbon therefore have different magnetic environments; each hydrogen is therefore coupled to the other hydrogen on the CH_2 bridge and to two different phosphorus centers.

The NMR spectral behavior is therefore consistent with the formulation of complex **6** as a bis(phosphine) complex of Rh(I) in which the long arms of the ligand **1** are able to span the *trans* positions of the square plane to form a 12-membered macrocyclic ring. This is favored by the affinity of Rh(I) for a P^{III} donor. It would be interesting to see if internal coupling reactions could

Table 8. ν_{CN} Shifts on Substitution

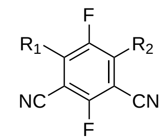

R_1/R_2	ν_{CN} (cm^{-1})	Δ (cm^{-1})[a]
F/F	2252	
F/N=PPh_3	2237	15
F/N=$P(Ph)_2CH_2PPh_2$	2231	21
N=PPh_3/N=PPh_3	2217	35
N=PPh_3/N=$P(Ph)_2CH_2PPh_2$	2214	38
N=$P(Ph)_2CH_2PPh_2$/ N=$P(Ph)_2CH_2PPh_2$	2205	47

[a] $\Delta = (2252 - \nu_{CN})\ cm^{-1}$.

be done within this structure as the resultant bicyclic ring structure should not suffer extraordinary strain; however, such experiments have not yet been attempted.

The stretching frequencies of the CN groups in the ligands are substantially reduced compared with those displayed by the starting material, 1,3-$(CN)_2C_6F_4$. These data are compared with that from other related compounds, such as 2,4-$(CN)_2C_6F_3N{=}PPh_3$,[23] 4,6-$(CN)_2C_6F_2$-1,3-bis(N=PPh_3),[23] and 2,4-$(CN)_2C_6F_3N{=}P(Ph)_2CH_2$-$PPh_2$[12] (Table 8) The order of Δ, the difference in ν_{CN} relative to the parent cyanobenzene, indicates that reducing the electronegativity of the substituent (or increasing the donor capability of the substituent) leads to more electron delocalization with CN groups and therefore a greater decrease of the CN stretching frequencies. N=$P(Ph)_2CH_2PPh_2$ is a better electron donor than N=PPh_3.

The influences of R_1 and R_2 on ν_{CN} are roughly additive. When R_1 = F, R_2 = (N=PPh_3), a decrease of 15 cm^{-1} for ν_{CO} is observed whereas when $R_1 = R_2$ = (N=PPh_3), the decrease is 35 cm^{-1}, which is slightly more than twice the value of the former. When R_1 = F, R_2 = (N=$P(Ph)_2CH_2PPh_2$), a decrease of 21 cm^{-1} is observed whereas when $R_1 = R_2$ = (N=$P(Ph)_2CH_2PPh_2$), the decrease is 47 cm^{-1}, which again is slightly more than twice the value of the former. In the case of R_1 = (N=PPh_3), R_2 = (N=$P(Ph)_2CH_2PPh_2$), a decrease of 38 cm^{-1} is observed, and this value is only slightly greater than the sum of the individual contribution of the two groups. Dividing these shift decrements into components due to each group gives an approximate decrement of 16−18 cm^{-1} for a N=PPh_3 group and approximately 24 cm^{-1} for the diphosphorus substituent relative to the original fluorine substituent.

Many complexes are known which contain uncoordinated CN groups, and there is no systematic shift of the CN stretching frequency; the value in the complex may be either higher or lower than that shown by the corresponding ligand.[24] We observe herein that the stretching frequencies of the uncoordinated CN groups in our metal complexes are in all cases higher than that of the corresponding vibration in the uncomplexed ligands (Table 2). Some shifts are very small; e.g. in the complex **4**, $\nu_{CN} = 2217\ cm^{-1}$, whereas, in ligand **2**, $\nu_{CN} = 2214\ cm^{-1}$, an increase of only 3 cm^{-1} upon

(23) Li,J.; Cavell, R. G. Manuscript in preparation.
(24) Storhoff, B. N.; Lewis, H. C., Jr. *Coord. Chem. Rev.* **1977**, *23*, 1.

coordination. The small shift indicates that the CN substituent environment is not greatly perturbed by coordination in this case. In contrast, for complex **5**, ν_{CN} =2227 cm^{-1}, an increase of 22 cm^{-1} upon complexation *vs* ligand **1** (ν_{CN} = 2205 cm^{-1}). Similarly the monometallic complex **6** (ν_{CN} = 2216 cm^{-1}) shows an increase of ν_{CN} relative to the ligand of 11 cm^{-1} which is just a half as large as the coordination shift in the bimetallic complex **5**. The difference between CN bond lengths in ligand **1** (1.140(6) Å) and in the metal complex **5** (1.12(1) Å) is not sufficiently great to indicate any trends or correlations between stretching frequency and bond length and strength.

Conclusions

Active fluorine atoms at the 4 and 6 positions, each *para* to the CN groups in 1,3-dicyanotetrafluorobenzene, can be substituted by an iminophosphorane unit; thus, mono- and disubstituted phosphorano-phosphinimine fluoroaromatic compounds can be obtained. The reactions proceed smoothly and can be carried out sequentially to yield complex bidentate phosphorano-phosphines. These multifunctional ligands readily react with $[Rh(CO)_2Cl]_2$ to form mono- and dimetallic Rh(I) complexes which exhibit either P−N chelate or P−P bidentate macrocyclic coordination. The dimetallic complex shows a square plannar geometry around each Rh(I) with the CO *cis* to the phosphine. The whole molecule has C_2 symmetry with the two fluorine atoms on a 2-fold axis. The structure of a P−P bidentate macrocyclic complex was deduced as a bis(phosphine) chelate from the complex second-order ^{31}P NMR spectrum solved by simulation. The two P^{III} centers are *trans* coordinated to the Rh center, and the two N atoms are not coordinated.

Experimental Section

All experimental manipulations were performed under atmosphere of dry argon using Schlenk techniques. Solvents were dried and distilled prior to use. Toluene, acetonitrile, and dichloromethane were distilled from Na, CaH_2, and P_4O_{10}, respectively. These solvents were purged with dry argon for at least 0.5 h before use. Commercial (Aldrich) supplies of dppm, Me_3SiN_3, 1,4-dicyanotetrafluorobenzene, 1,3-dicyanotetrafluorobenzene, and 1,2-dicyanotetrafluorobenzene were used as obtained. $Ph_2PCH_2P(Ph)_2$=NSiMe$_3$ was prepared as previously described.[1] Nuclear magnetic resonance spectra were recorded on Bruker WH-200 and 400 spectrometers with reference to the deuterium signal of the solvent employed. The ^{1}H chemical shifts are reported in ppm from external Me_4Si, the ^{31}P NMR spectra are reported in ppm from external 85% H_3PO_4, and the ^{19}F NMR spectra are reported in ppm from external $CFCl_3$. Positive values reflect shifts downfield. Low-resolution mass spectra were recorded at 16 or 70 eV on an AEI MS50 spectrometer. Positive ion fast atom bombardment mass spectra (FAB-MS) were recorded by using Xe fast atoms on a customized AEI MS9 spectrometer. Infrared spectra were recorded on a Nicolet 7199 infrared spectrometer. Melting points were ascertained by visual methods in unsealed capillaries. Osmometry measurements were made in CH_2Br_2 solutions on a Corona Wescan vapor pressure osmometer by the University of Alberta Microanalytical Services.

Synthesis of 4,6-(CN)$_2$C$_6$F$_2$-1,3-bis(N=P(Ph)$_2$CH$_2$PPh$_2$) (1). To a solution of Me_3SiN=P(Ph)$_2$CH$_2$PPh$_2$ (0.80 g; 1.70 mmol) in dry toluene (20 mL) was added dropwise a solution of 1,3-dicyanotetrafluorobenzene (0.17 g; 0.85 mmol) also in toluene (20 mL). The reaction mixture was refluxed for 12 h before the solvent was removed *in vacuo* to leave a yellow crystalline solid. This crude product was recrystallized from acetonitrile to obtain the pure compound **1** (yield 0.32 g; 39%; cubic crystals, suitable for diffraction studies; mp 292 °C). Anal. Calcd for $C_{58}H_{44}N_4F_2P_2$: C, 72.65; H, 4.62; N, 5.84. Found: C, 72.37; H, 4.50; N, 5.85. MS (FAB, *m/z*): 959 (M$^+$, 100%). ^{1}H NMR (CDCl$_3$): phenyl rings δ 7.05, 7.15, 7.30, 7.42, 7.75 (m, 40H); PCH$_2$P methylene δ 2.77 (dd, 2H, $^2J_{HP^V}$ = 12.40 Hz, $^2J_{HP^{III}}$ = 2.30 Hz).

Synthesis of 4,6-(CN)$_2$C$_6$F$_2$-1-(N=P(Ph)$_2$CH$_2$P(Ph)$_2$)-3-(N=PPh$_3$) (2). To a solution of Me_3SiN=P(Ph)$_2$CH$_2$PPh$_2$ (0.31 g; 0.66 mmol) in dry toluene (20 mL) was added dropwise a solution of 2,4-(CN)$_2$C$_6$F$_3$N=PPh$_3$[23] (0.30 g; 0.66 mmol) also in toluene (50 mL). The reaction mixture was refluxed for 12 h before the solvent was removed *in vacuo* to leave a light yellow crystalline solid. This crude product was recrystallized from acetonitrile to obtain the pure compound **2** (yield 0.52 g; 95%; cubic crystals, suitable for diffraction studies; mp 231 °C). Anal. Calcd for $C_{51}H_{37}N_4F_2P_3$: C, 73.20; H, 4.47; N, 6.70. Found: C, 72.67; H, 4.37; N, 6.74. MS (EI, *m/z*): 836 (M$^+$, 100%). ^{1}H NMR (CDCl$_3$): phenyl rings δ 7.10, 7.35, 7.55 (m, 35H), PCH$_2$P methylene δ 2.83 (dd, 2H, $^2J_{HP^V}$ = 12.50 Hz, $^2J_{HP^{III}}$ = 2.30 Hz).

Synthesis of 4,6-(CN)$_2$C$_6$F$_2$-1-(N=PPh$_2$CH$_2$PPh$_2$)-3-(N=PPh$_2$Me) (3). To a solution of Me_3SiN=PPh$_2$CH$_2$PPh$_2$ (0.30 g; 0.63 mmol) in dry toluene (20 mL) was added dropwise a solution of 2,4-(CN)$_2$C$_6$F$_3$N=PPh$_2$Me[23] (0.25 g; 0.63 mmol) also in toluene (60 mL). The reaction mixture was refluxed for 12 h before the solvent was removed *in vacuo* to leave a light yellow crystalline solid. This crude product was recrystallized from acetonitrile to obtain the pure compound **3** (yield 0.35 g; 74%; colorless cubic crystals, suitable for diffraction studies; mp 241 °C). Anal. Calcd for $C_{46}H_{35}N_4F_2P_3$: C, 71.32; H, 4.55; N, 7.23. Found: C, 71.09; H, 4.56; N, 7.47. MS (EI, *m/z*): 775 (M$^+$, 100%). ^{1}H NMR (CDCl$_3$): phenyl rings δ 7.15, 7.28, 7.45, 7.70 (m, 20H), methyl group δ 1.63 (dd, 3H). PCH$_2$P methylene δ 2.91 (dd, 2H, $^2J_{HP^V}$ = 12.40 Hz, $^2J_{HP^{III}}$= 2.50 Hz).

Synthesis of 4,6-(CN)$_2$C$_6$F$_2$-3-(N=PPh$_3$)-1-(N=P(Ph)$_2$CH$_2$-P(Ph)$_2$Rh(CO)Cl) (4). To a solution of $[Rh(CO)_2Cl]_2$ (30.0 mg; 0.07714 mmol) in dry CH_2Cl_2 (15 mL) was added dropwise a solution of 4,6-(CN)$_2$C$_6$F$_2$-1-(N=P(Ph)$_2$CH$_2$PPh$_2$)-3-(N=PPh$_3$) (**2**) (0.1291 g; 0.1543 mmol) also in CH_2Cl_2 (20 mL). The reaction mixture was stirred at room temperature for 4 h before the solvent was removed *in vacuo* to leave a yellow solid. This crude product was recrystallized from CH_2Cl_2/hexane (2:1) to obtain the pure compound **4** (yield 0.134 g; 87%; mp > 210 °C dec). Anal. Calcd for $C_{52}H_{37}N_4OClF_2P_3Rh$: C, 62.26; H, 3.72; N, 5.58; Cl, 3.53. Found: C, 62.23; H, 3.65; N, 5.60; Cl, 3.96. MS (FAB, *m/z*): 1003 (M$^+$, 100%). ^{1}H NMR (CDCl$_3$): phenyl rings δ 7.25, 7.53, 7.68, 7.85 (m, 35H), PCH$_2$P methylene δ 2.91 (d, 2H, $^2J_{HP^V}$ = 12.00 Hz).

Synthesis of 4,6-(CN)$_2$C$_6$F$_2$-1,3-bis(N=P(Ph)$_2$CH$_2$P-(Ph)$_2$Rh(CO)Cl) (5). Method A. To a solution of $[Rh(CO)_2Cl]_2$ (30.0 mg; 0.077 mmol) in dry CH_2Cl_2 (15 mL) was added dropwise a solution of 4,6-(CN)$_2$C$_6$F$_2$-1,3-bis(N=P(Ph)$_2$CH$_2$-PPh$_2$) (**1**) (0.0740 g; 0.077 mmol) also in CH_2Cl_2 (25 mL). The reaction mixture was stirred at room temperature for 4 h before the solvent was removed *in vacuo* to leave a yellow solid. This crude product was recrystallized from CH_2Cl_2/hexane (2:1) to obtain the dichloromethane solvate of **5** (yield 64.0 mg; 60%; mp 276−8 °C). Anal. Calcd for $C_{61}H_{46}N_4O_2Cl_4F_2P_4Rh_2$: C, 53.22; H, 3.37; N, 4.07; Cl, 10.30. Found: C, 53.11; H, 3.24; N, 4.06; Cl, 9.47. MS (FAB, *m/z*): 1255 ((M$^+$ − Cl), 100%). No peak at *m/z* 1292 (parent peak) was observed. ^{1}H NMR (CDCl$_3$): phenyl rings δ 7.15, 7.30, 7.50, 7.80 (m, 40H), PCH$_2$P methylene δ 3.77 (m, 2H), δ 3.55 (m, 2H). **Method B.** To a 50 mL flask was added 10 mL of CH_2Cl_2, compound **6** (0.037 g, 0.0306 mmol), and $[Rh(CO)_2Cl]_2$ (0.001 g, 0.0153 mmol). The mixture was stirred at room temperature for 5 h before the solvent was removed *in vacuo* to leave **5** as a yellow solid identified by ^{31}P, and ^{19}F NMR and IR data.

Synthesis of 4,6-$(CN)_2C_6F_2$-1,3-bis(N=P(Ph)$_2$CH$_2$P-(Ph)$_2$)Rh(CO)Cl (6). Method A. To a solution of $[Rh(CO)_2Cl]_2$ (30.0 mg; 0.077 mmol) in dry CH_2Cl_2 (15 mL) was added dropwise a solution of 4,6-$(CN)_2C_6F_2$-1,3-(N=P(Ph)$_2$CH$_2$P(Ph)$_2$)$_2$ (**1**) (0.1480 g; 0.154 mmol) also in CH_2Cl_2 (35 mL). The reaction mixture was stirred at room temperature for 4 h before the solvent was removed *in vacuo* to leave a yellow solid. This crude product was recrystallized from CH_2Cl_2/hexane (2:1) to obtain the dichloromethane solvates of **6** (yield 0.117 g; 63%; mp dec). Anal. Calcd for $C_{60}H_{46}N_4OCl_3F_2P_4Rh$: C, 59.55; H, 3.83; N, 4.63; Cl, 8.79. Found: C, 59.55; H, 3.58; N, 4.69; Cl, 8.80. MS (FAB, *m*/*z*): 1125 (M^+, 100%). Molecular weight determination: 1041. ^1H NMR ($CDCl_3$): phenyl rings δ 7.30, 7.57 (m, 40H), PCH_2P methylene δ 3.38 (ddd, 2H), δ 5.35 (ddd, 2H). **Method B.** To a 50 mL flask was added 10 mL of CH_2Cl_2, compound **1** (0.012 g, 0.013 mmol), and compound **5** (0.017 g, 0.013 mmol). The mixture was stirred at room temperature for 5 h before the solvent was removed *in vacuo* to leave a yellow solid which was identified as **6** by ^{31}P, and ^{19}F NMR and IR data.

Crystallography. Crystal structures of the compounds **1**, **2**, and **5** were done at the University of Alberta. The relevant experimental collection and solution data are given in Table 3. In all cases the data collection and structure refinement was straightforward. Direct methods were used to solve all structures. The hydrogen atoms were generated at idealized calculated positions by assuming a C−H bond length of 0.95 Å and the appropriate sp^2 or sp^3 geometry. All hydrogen atoms were then included in the calculations with fixed, isotropic Gaussian displacement parameters 1.2 times those of the attached atoms and were constrained to "ride" on the attached atoms. Final *R* values are given in Table 3, and final difference peaks were small and without chemical significance.

Acknowledgment. We thank the Natural Sciences and Engineering Research Council of Canada and the University of Alberta for financial support.

Supporting Information Available: For **1**, tables of crystallographic experimental data (S1-1), atomic coordinates and equivalent isotropic displacement parameters (S1-2), selected interatomic distances (S1-3), selected interatomic angles (S1-4), torsional angles (S1-5), least-squares planes (S1-6), anisotropic displacement parameters (S1-7), and derived atomic coordinates and displacement parameters for hydrogen atoms (S1-8), for **2**, tables of crystallographic experimental data (S2-1), selected interatomic distances (S2-2), selected interatomic angles (S2-3), torsional angles (S2-4), weighted least-squares planes and dihedral angles (S2-5), atomic coordinates and equivalent isotropic displacement parameters (S2-6), anisotropic displacement parameters (S2-7), and derived atomic coordinates and displacement parameters for hydrogen atoms (S2-8), and for **5**, tables of crystallographic experimental data (S3-1), selected interatomic distances (S3-2), selected interatomic angles (S3-3), torsional angles (S3-4), weighted least-squares planes (S3-5), atomic coordinates and equivalent isotropic displacement parameters (S3-6), anisotropic displacement parameters (S3-7), and derived atomic coordinates and displacement parameters for hydrogen atoms (S3-8) (49 pages). Ordering information is given on any current masthead page.

OM950767D